







Article

# mmWave Four-Element MIMO Antenna for Future 5G Systems

Muhammad Abbas Khan <sup>1</sup>, Abdullah G. Al Harbi <sup>2</sup> , Saad Hassan Kiani <sup>3,4,\*</sup> , Anis Nurashikin Nordin <sup>5</sup> , Mehr E Munir <sup>6</sup>, Sohail Imran Saeed <sup>6</sup>, Javed Iqbal <sup>7,8</sup> , Esraa Mousa Ali <sup>9</sup>, Mohammad Alibakhshikenari <sup>10</sup>  and Mariana Dalarsson <sup>11,\*</sup> 

- <sup>1</sup> Department of Electrical Engineering, Balochistan University of Information Technology, Engineering and Management Sciences, Quetta 87300, Pakistan; muhammad.abbas@buitms.edu.pk
  - <sup>2</sup> Department of Electrical Engineering, Faculty of Engineering, Jouf University, Sakaka 42421, Saudi Arabia; a.g.alharbi@ieee.org
  - <sup>3</sup> Department of Electrical Engineering, IIC University of Technology, Phnom Penh 121206, Cambodia
  - <sup>4</sup> Smart Systems Engineering Laboratory, College of Engineering, Prince Sultan University, Riyadh 11586, Saudi Arabia
  - <sup>5</sup> Department of Electrical & Computer Engineering, International Islamic University Malaysia, Kuala Lumpur 43200, Malaysia; anisnn@iiu.edu.my
  - <sup>6</sup> Department of Electrical Engineering, Iqra National University, Peshawar 25000, Pakistan; mehre.munir@inu.edu.pk (M.E.M.); sohail.imran@inu.edu.pk (S.I.S.)
  - <sup>7</sup> Department of Electrical Engineering, Faculty of Engineering and Technology, Gomal University, Dera Ismail Khan 29050, Pakistan; javediqbal.iet@gu.edu.pk
  - <sup>8</sup> School of Electrical and Electronic Engineering, Engineering Campus, Universiti Sains Malaysia, Nibog Tebal 14300, Malaysia
  - <sup>9</sup> Faculty of Aviation Sciences, Amman Arab University, Amman 11953, Jordan; esraa\_ali@aau.edu.jo
  - <sup>10</sup> Department of Signal Theory and Communications, Universidad Carlos III de Madrid, Leganés, 28911 Madrid, Spain; mohammad.alibakhshikenari@uc3m.es
  - <sup>11</sup> School of Electrical Engineering and Computer Science, KTH Royal Institute of Technology, SE 100-44 Stockholm, Sweden
- \* Correspondence: iam.kiani91@gmail.com (S.H.K.); mardal@kth.se (M.D.)



**Citation:** Khan, M.A.; Al Harbi, A.G.; Kiani, S.H.; Nordin, A.N.; Munir, M.E.; Saeed, S.I.; Iqbal, J.; Ali, E.M.; Alibakhshikenari, M.; Dalarsson, M. mmWave Four-Element MIMO Antenna for Future 5G Systems. *Appl. Sci.* **2022**, *12*, 4280. <https://doi.org/10.3390/app12094280>

Academic Editor: Hosung Choo

Received: 7 April 2022

Accepted: 22 April 2022

Published: 23 April 2022

**Publisher's Note:** MDPI stays neutral with regard to jurisdictional claims in published maps and institutional affiliations.



**Copyright:** © 2022 by the authors. Licensee MDPI, Basel, Switzerland. This article is an open access article distributed under the terms and conditions of the Creative Commons Attribution (CC BY) license (<https://creativecommons.org/licenses/by/4.0/>).

**Abstract:** This paper presents an S-shape four-port Multiple Input Multiple Output (MIMO) wide-band mmWave antenna with bandwidth of 25 GHz to 39 GHz. The antenna is designed on 0.254 mm ultra-thin RO5880 with permittivity of 2.3. The dimensions of proposed S-shape antenna are 10 × 12 mm for single element and 24 × 24 mm for four-port MIMO configuration. A decoupling network is introduced to further compress mutual coupling among MIMO elements. The peak gain achieved is 7.1 dBi and MIMO assembly delivers diversity scheme. The proposed MIMO antenna is fabricated, and simulated results are found to be in excellent agreement with simulations. Through the results obtained, the proposed MIMO antenna system can be considered as a potential candidate for future mmWave devices.

**Keywords:** mmWave; four port; MIMO; gain; ECC diversity

## 1. Introduction

The new era of communication technology has enabled 5th Generation (5G)-driven systems that allow for high-speed data rates with enhanced bandwidth and low latencies. Compared to its predecessor, 4th Generation (4G) systems framework, 5G technology standards offer higher data rates of up to 1 Giga bit/s. Furthermore, 5G systems can be divided into two categories, namely, Sub GHz and mmWave regions, where mmWave is more promising for high-data-rate transmission and to support future cellular devices. The mmWave band of 5G offers a starting frequency of 24 GHz and above, offering much potential. Within the mmWave band, antenna designers have created novel shapes and assemblies. In addition, 28 GHz, 33 GHz and 37 GHz are the bands in mmWave which have drawn antenna designers' attention and have been introduced with these novel shapes and

assemblies [1,2]. MIMO antennas have given a new direction to wireless communication and have become very attractive for 5G applications [3,4]. A MIMO Antenna offers pattern and spatial diversity characteristics, hence enabling better signal reception and data transmission. Designing a compact 5G MIMO antenna is still a challenging task in the current scenario, since accommodating a higher number of antenna elements together gives rise to coupling effects, which affect antenna performance characteristics. As today's cellular providers attempt to deliver high-quality, low-latency video and multimedia applications for wireless devices, they are limited to a carrier frequency spectrum ranging between 700 MHz and 2.6 GHz [5].

In open literature, a lot of MIMO antennas have been proposed in the mmWave spectrum, targeting different licensed and unlicensed frequencies [6–12]. In [6], a Substrate-Integrated Waveguide (SIW) antenna is presented, covering a frequency from 57 to 71 GHz for mmWave 5G and short-range radar applications. Although the presented antenna is well-designed, with small size of  $28 \times 28$  mm, the compact design is difficult to manufacture due to multilayer assembly and bonding films. Planar antennas are simple and easy to design compared to SIW antenna systems. In [7], a simple planar infinity shell-shape antenna is presented in four-port MIMO configuration; the proposed antenna delivers a bandwidth of 8 GHz, approximately. Similarly, in [8], a nature-inspired four-port MIMO antenna is presented with a bandwidth ranging to 7 GHz with central frequency of 28 GHz. The size of the antenna is  $30 \times 30$  mm, and it provides pattern and spatial diversity characteristics. In [9], a tree-shaped four-port MIMO antenna is presented. The antenna provides wideband characteristics of 23–40 GHz while providing peak isolation of 22 dB. The size of the proposed MIMO antenna is  $80 \times 80$  mm, which is large enough to be embedded in mmWave circuits. A four-port Dielectric Resonator Antenna (DRA) in [10] provides the bandwidth of 2.23 GHz, ranging from 26.7 to 28.1 GHz. The size of the antenna is  $20 \times 40$  mm and antenna isolation has been improved up to a peak value of 22 dB by inserting metamaterial, but introducing metamaterial overall increased the complexity of antenna systems. In [11], an E-Shape H slotted dual-band four-port MIMO antenna is reported. The antenna offers good compact dimensions of  $24 \times 24$  mm but the reported bandwidth is too low. In [12], a four-port MIMO antenna system is reported providing bandwidth characteristics of 36.83–40.0 GHz. The antenna is simple in structure but provides low bandwidth.

Therefore, this work was intended to design an MIMO antenna that is small in size, covers a wide bandwidth and offers high isolation characteristics throughout the desired resonance bandwidth. The proposed antenna is simple in shape and provides wideband characteristics of almost 15 GHz, with a better isolation value of  $-26$  dB. The isolation level has been improved by inserting a line resonator.

This paper's layout is as follows: Section 1 covers the literature on MIMO antenna systems presented in open literature. Section 2 covers the antenna's design characteristics step-by-step and its MIMO configuration. Section 3 discusses the results obtained from the fabricated prototype with simulated results. Concluding remarks are given at the end.

## 2. Antenna Design

### 2.1. Single Element

The proposed antenna is designed based on an ultra-thin 0.254 mm RO5880 substrate with relative permittivity of 2.3. The antenna has an overall length and width of  $12 \times 10$  mm. The antenna comprises three strips closely connected to each other with 0.35 mm strips at top-right and bottom-left sides. Figure 1 shows the proposed S-shape antenna design, front and back, in detail. The ground plane consists of a square-shape slot incorporated at the top-middle side. Figure 2 explains the evolution of design through three different steps. To attain the anticipated resonance, the proposed single-monopole antenna element is attained with insertion of stubs. These stubs are then parametrically optimized for achieving optimum response.

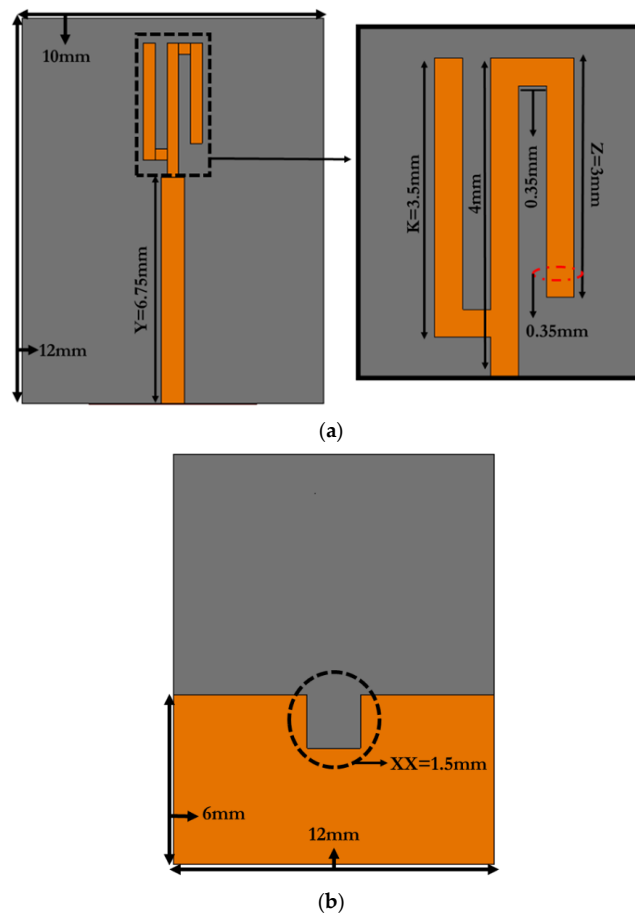


Figure 1. Proposed Antenna (a) Front (b) Back.

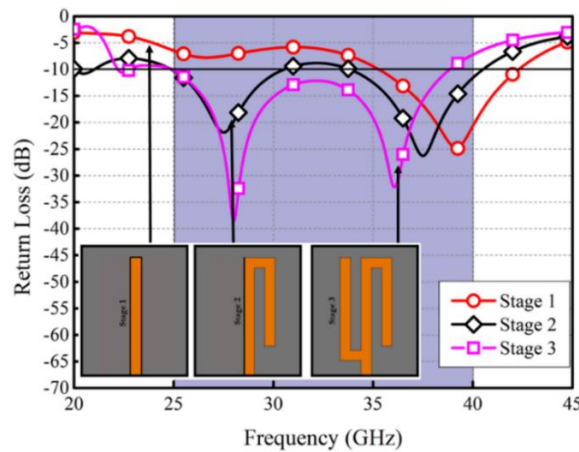


Figure 2. Design Evolution of the proposed Antenna.

In stage 1, a simple l-shape resonator was introduced that showed the resonance response from 36 to 42 GHz with central frequency of 39 GHz. This was further modified with the insertion of an inverted L-shape stub on the right hand side of the l-shape strip. The stub enhanced the bandwidth response to dual-band characteristics, which in stage 3 was modified to a wide bandwidth with the insertion of L-shape stub on left side of the resonating structure.

The proposed MIMO antenna has been evolved in number of parametric steps. Parametrical studies are conducted to see the antenna’s resonance response by altering different paths of currents. Figure 3 shows the wideband response achieved through

different parametrical studies conducted. The parameters optimized were Z, Y, K and XX. At the start, parameter Z was parametrically optimized. The starting value was kept at 2 mm and was analyzed up to 4 mm. Five different values in this range were analyzed, each with a difference of 0.5 mm. It was observed that with every increment in value, the design response changed rapidly. It was observed that the resonance value increases with every increment in parameter Z. At 2 mm, a resonance of nearly 7 GHz was achieved from 31 to 38 GHz. At 2.5 mm, the resonance starts at 27 GHz and ends at 38 GHz, giving an approximately 11 GHz bandwidth. The optimal response was achieved at 3 mm, from 25 to 39 GHz. After this optimum value, any further increase resulted in effecting the resonance response. From Figure 3a, it can be seen that the resonances become abrupt. Similarly, in Figure 3b, parameter Y, which is feed length, was analyzed with five samples from 6.25 to 7.25 mm. The optimum response was achieved at 6.25 mm. With further increases in length, the resonance response shifted backwards. The K parameter in Figure 3c showed the optimal response at 3.5 mm. Any further increases and decreases showed that although the resonance bandwidth remains uncertain, the reflection coefficient value becomes abrupt. The trunked ground-plane square slot was optimized from 1.3 to 1.7 mm. The length and width of the square slot was kept same, and Figure 3d shows resonance behavior with antenna parameter XX. Figure 4 shows the single-element radiation patterns and gain over frequency. The gain ranges between 3.9 and 5.2 and efficiency ranges between 85 and 98%.

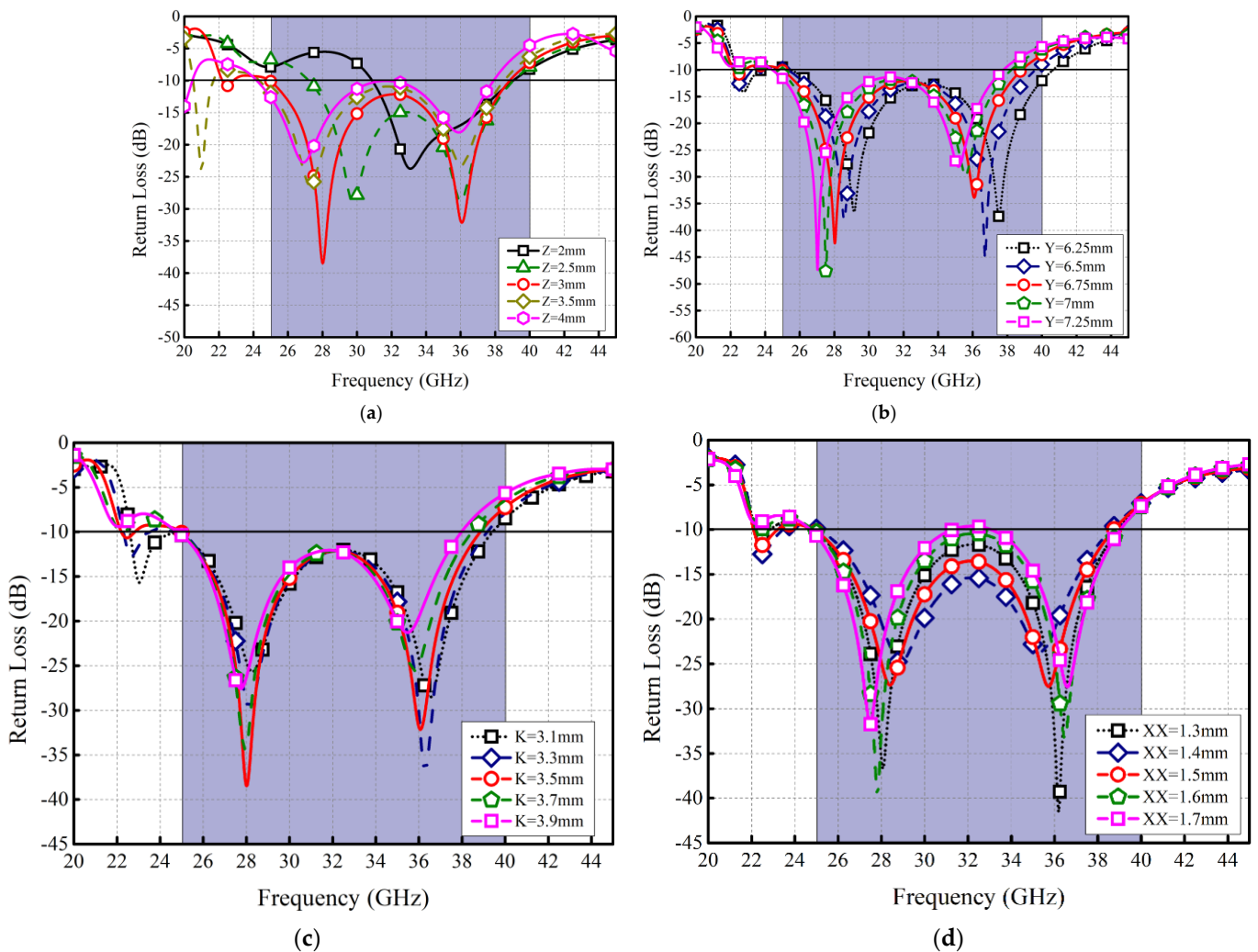


Figure 3. Parametric Studies conducted (a) Z (b) Y (c) K (d) XX.

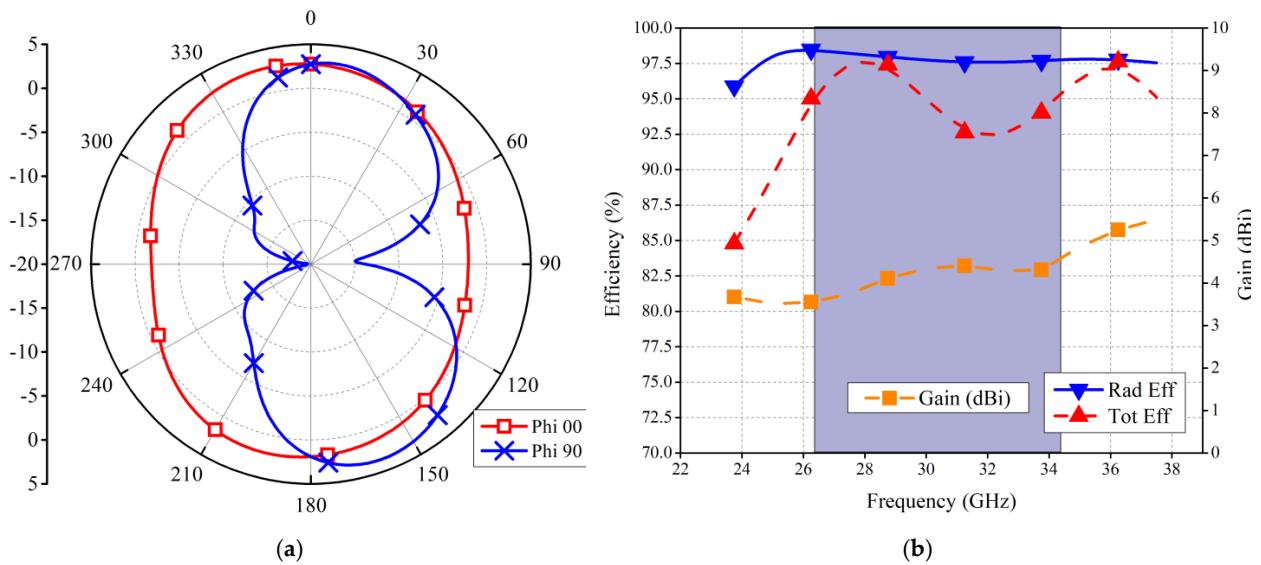


Figure 4. Single-Element Performance Parameters (a) Radiation Patterns (b) Gain and Efficiency.

### 2.2. MIMO Antenna Configuration

The S-shape antenna was extended to four-element MIMO configuration. The total size of the antenna was kept at 24 mm × 24 mm. The MIMO antennas are arranged orthogonal to each other. Additionally, as in MIMO antennas, the isolation values play vital role.

Therefore, in order to enhance isolation and decrease the mutual coupling among radiating elements, an isolating structure is introduced in between four radiating elements. The proposed isolating structure consists of a tilted square small patch with extended arms at each side. Figure 5 shows the MIMO antenna design with isolating structure.

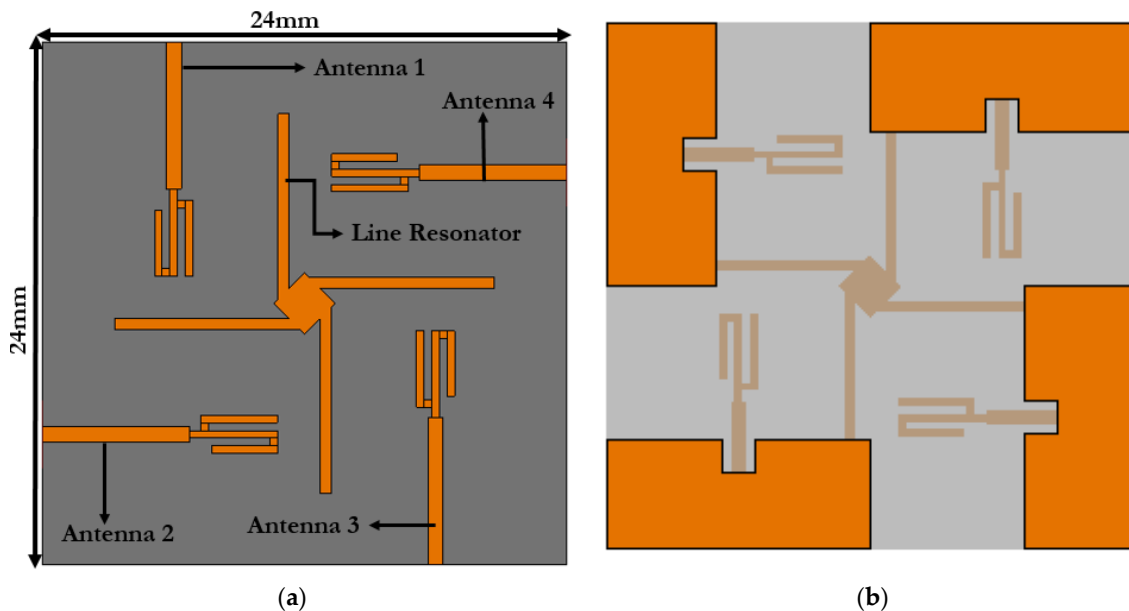


Figure 5. MIMO Antenna (a) Front (b) Back.

### 3. Experimental Results

The proposed MIMO antenna was fabricated using a Leiterplatten-Kopierfräsen, LPFK, machine, and was tested in anechoic chamber. Due to symmetricity of the design, only one side of the proposed antenna is tested. Figure 6 shows the proposed antenna structure's

copper layer with 2.4 mm end launch connectors. The antenna has been set with a scale to show the physical length of the proposed prototype.



Figure 6. Fabricated Prototype.

Figure 7 shows the isolation of the proposed antenna with and without the isolating structure. It can clearly be seen that with the insertion of a line resonator at the center, the resonator acts as a decoupling structure for MIMO antennas as the line resonator effectively cancels the constructive interference of currents among radiating elements, and thus the isolation levels are improved.

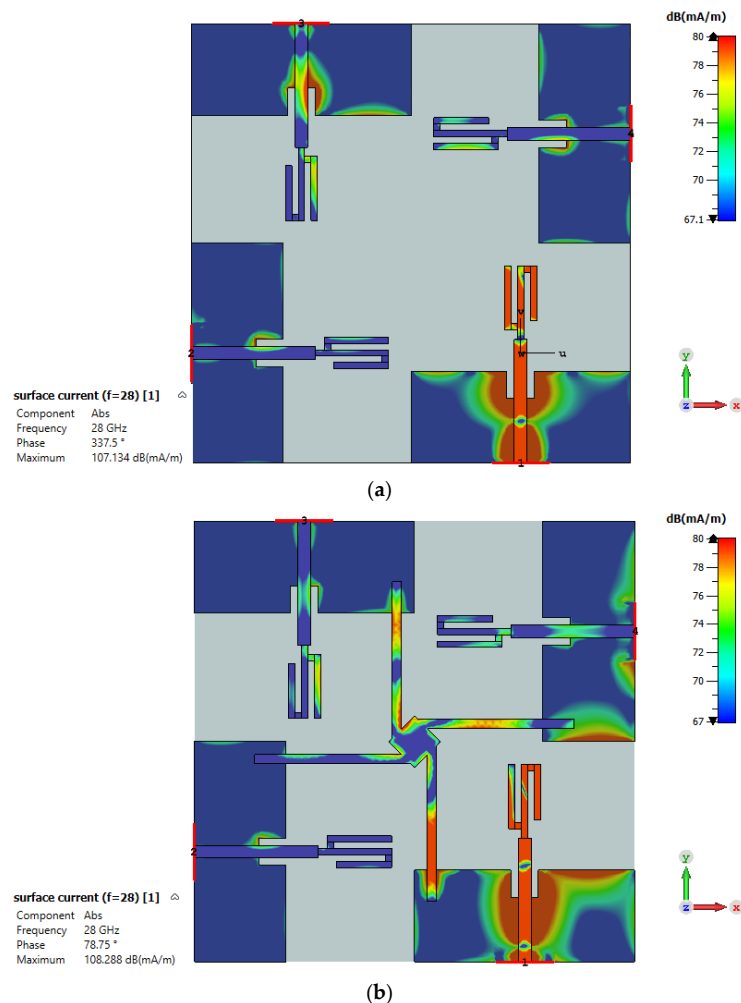


Figure 7. Surface Current Distribution (a) Without Isolating Structure (b) With Isolating Structure.

Furthermore, the simulated and measured S-parameters are shown in Figure 8. The reflection coefficient in Figure 8a shows the resonance from 22 to 40 GHz, while the isolation value of antenna 1 and antenna 3 is found to be in between  $-15$  dB and  $-19$  dB without the presence of decoupling structure. The lowest isolation without decoupling structure is found to be  $-19$  dB at 29 GHz frequency. As with the insertion of decoupling structure, the isolation value improved from  $-22$  dB to  $-27$  dB. The isolation value with decoupling structure showed improvement up to 5 dB for antenna 1 and antenna 3. The isolation value between adjacent radiating elements, antenna 1 and antenna 2 was also improved. The measured results achieved after measurements are shown to be in excellent agreement with the simulations. A few minor alterations can be seen but can be attributed to errors during measurement set up.

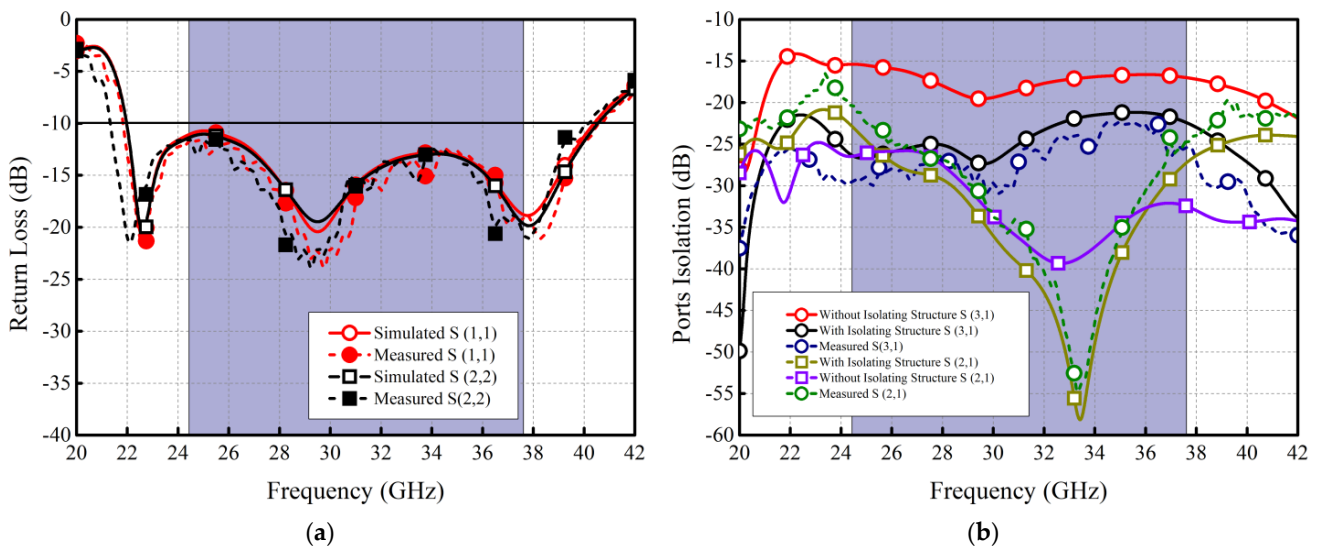


Figure 8. Simulated and Measured S-Parameters. (a) Return loss (b) Ports Isolation.

Figure 9 shows the antenna efficiency and simulated and measured gain of the proposed MIMO system. The efficiency of the MIMO antenna ranges in between 85% and 94%, while at 28 GHz, the efficiency is found to be almost 92 to 92.5% for all radiating elements. The range of the antenna gain is found to be 5.9 to 7 dB.

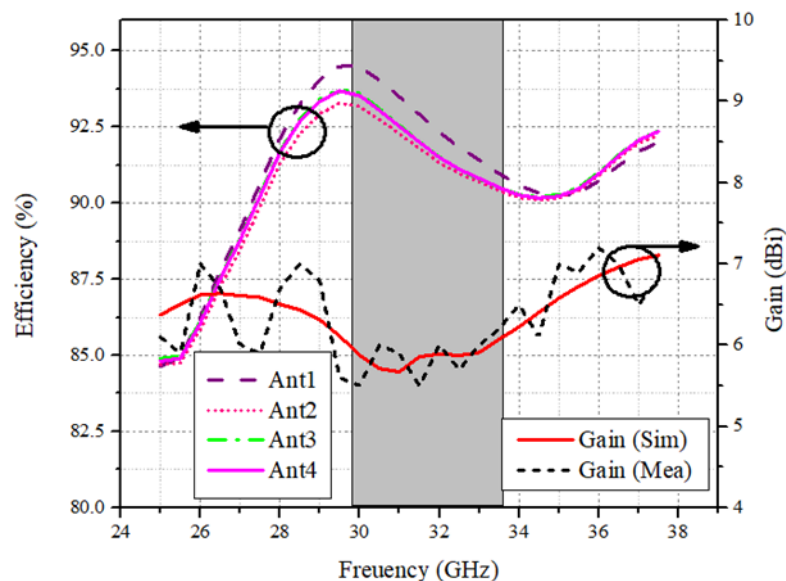


Figure 9. Efficiency and Gain of the MIMO Antenna.

The radiation patterns both in the 2D and 3D plane are shown in Figure 10. The patterns of antenna 1 and antenna 2 are shown and discussed. The 28 GHz frequency patterns are shown at  $\Phi = 90$ ,  $\Phi = 0$  and  $\Theta = 90$  Plane. As seen from the figure, the proposed antenna system shows pattern and spatial diversity characteristics. The 3D patterns at 28 GHz are also shown in Figure 10. The gain ranges from 6.4 to 7.1 dB for all four radiating elements.

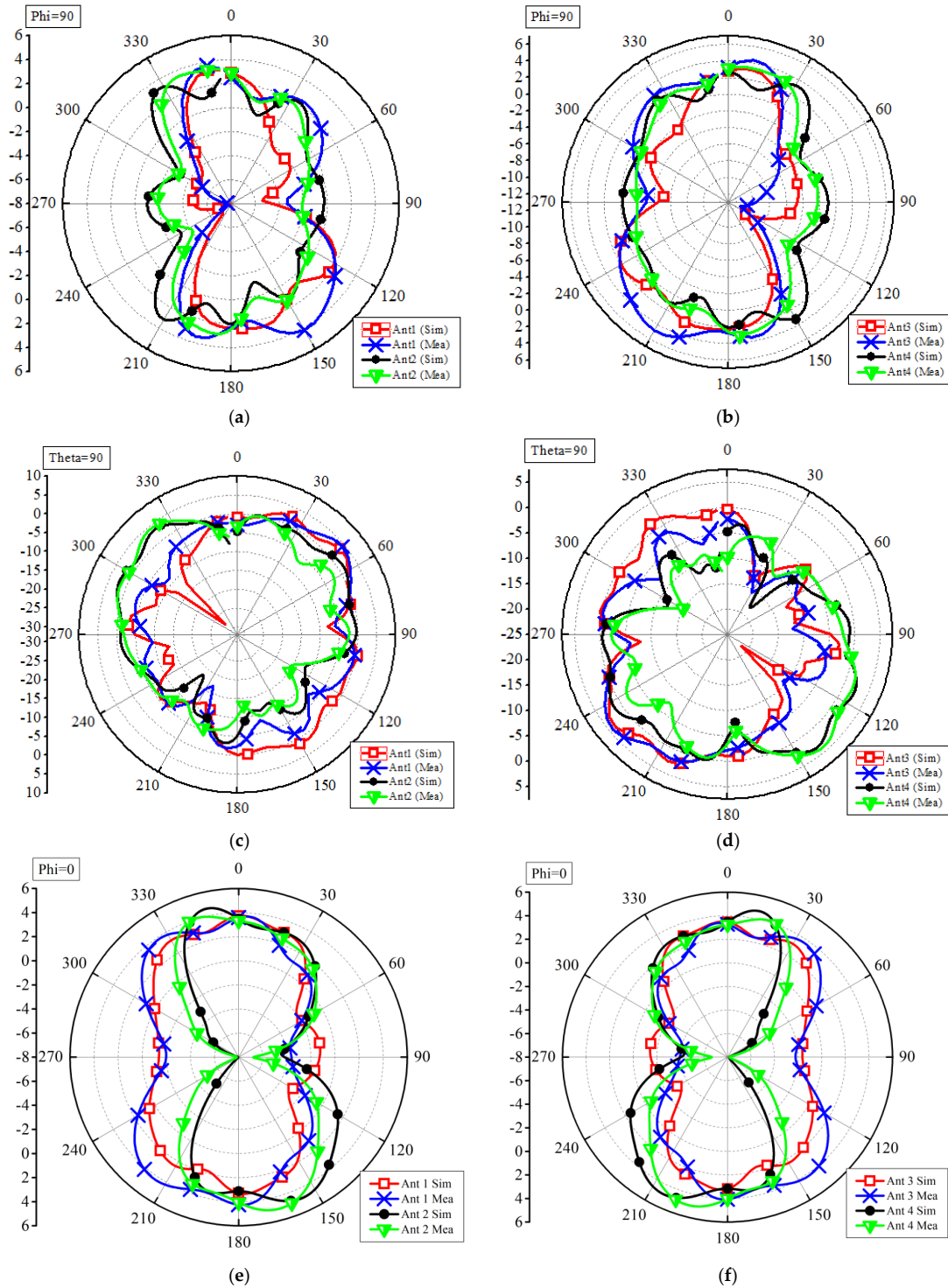
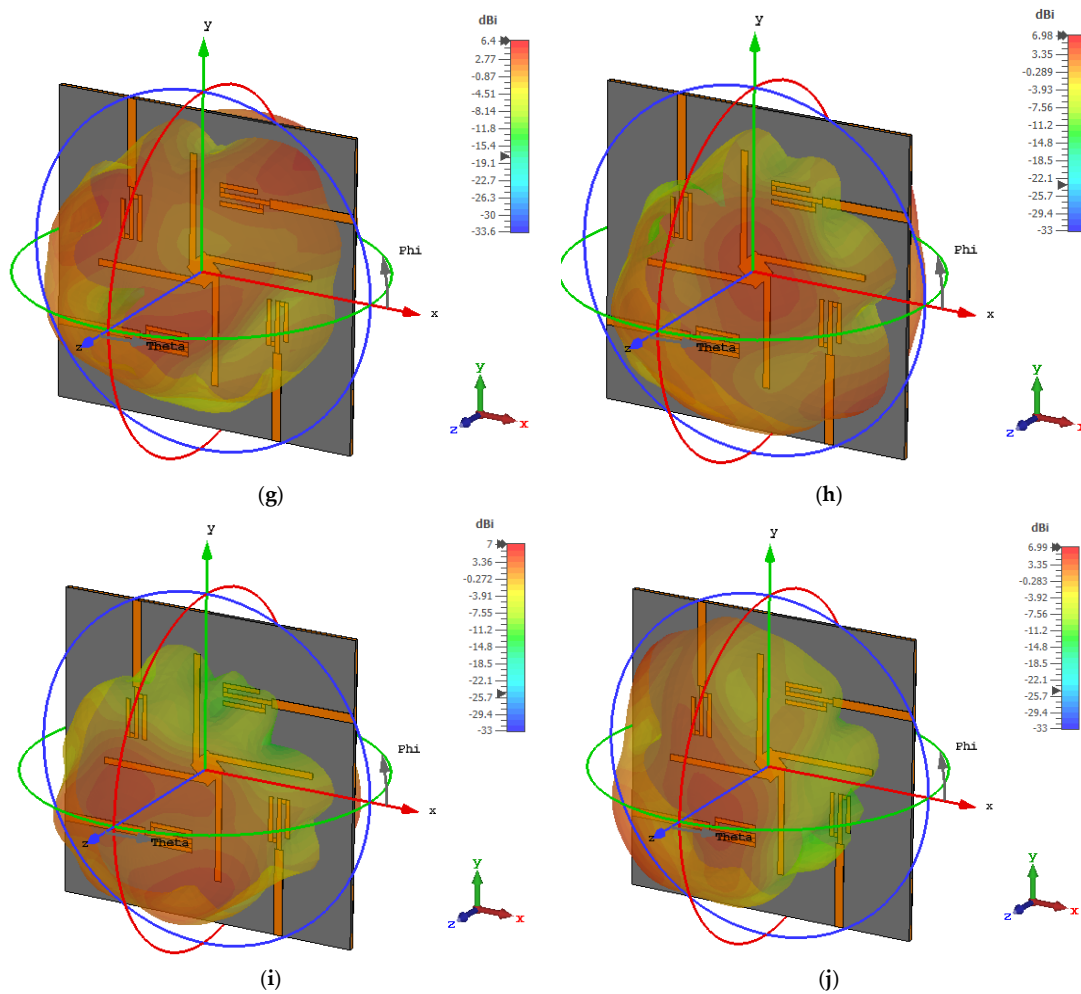


Figure 10. Cont.





**Figure 10.** Radiation Patterns (a) 2D antenna 1 and antenna 2 Phi90 (b) 2D antenna 3 and antenna 4 Phi90 (c) 2D antenna 1 and antenna 2 Theta 90 (d) 2D antenna 3 and antenna 4 Theta90 (e) 2D antenna 1 and antenna 2 Phi0 (f) 2D antenna 3 and antenna 4 Phi0 (g) 3D antenna 1 (h) 3D antenna 2 (i) 3D antenna 3 (j) 3D antenna 4.

*MIMO Parameters*

MIMO parameters are important to discuss while designing an MIMO antenna system. These MIMO parameters include Envelope Correlation coefficient (ECC) and Mean Effective Gain (MEG). ECC is the measure of how well the antennas are isolated. Ranging from 0 to 1, an ECC of less than 0.5 shows that antennas are well-isolated. Figure 11 shows the ECC of the proposed MIMO system. The ECC obtained has been calculated using far-field results from the MIMO system. The equations used for calculating ECC and MEG have been derived from [13–15]. From the figure, it can clearly be seen that the ECC of the proposed MIMO system is less than <math>0.01</math> throughout the band of interest.

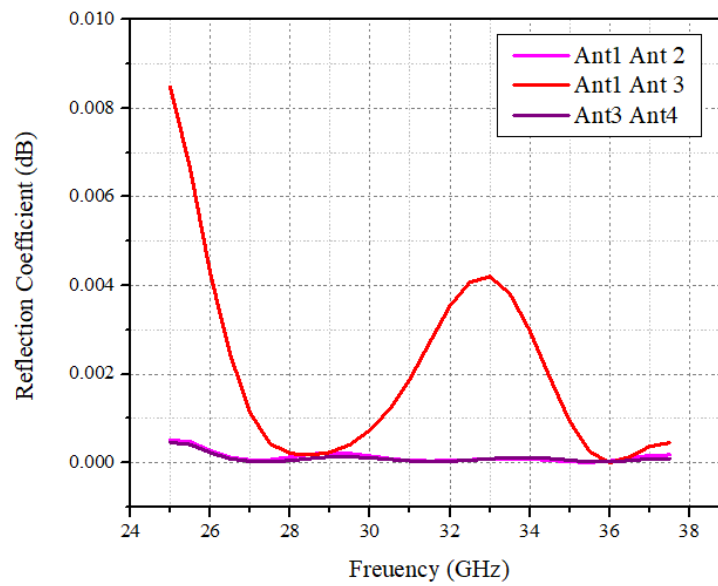


Figure 11. ECC derived.

The mean effective gain (MEG) is an ability of an antenna in a multipath environment to receive electromagnetic power. The MEG of the proposed MIMO antenna is given in Table 1. Through Table 1, the MEG of the proposed antenna system satisfies the MIMO performance, exhibiting good channel characteristics.

Table 1. Mean Effective Gain of the proposed Antenna at 28 and 29 GHz Frequency.

Frequency (GHz)	MEG1	MEG2	MEG3	MEG4
28	−3.50	−3.21	−3.26	−3.10
29	−2.99	−3.06	−3.61	−3.11

Table 2 shows a comparison of the proposed MIMO antenna with the proposed MIMO antenna system. The authors in [16–18] also present folk-shape structures, however, none of them resonate at the mmwave region and cover UWB characteristics from 3 to 12 GHz. Additionally, one study [16] shows some notching features. From the comparison table, it can be seen that our proposed MIMO system is compact in size compared to those in the published literature, and offers good performance MIMO characteristics.

Table 2. Proposed Four-Element MIMO Antenna comparison with published literature.

Refs.	Ant. Elements	Single Element (mm <sup>2</sup> )	Array (mm <sup>2</sup> )	Bandwidth	Isolation (dB)	Efficiency (%)	ECC
[7]	4	12 × 10	30 × 30	27–30	28	84	<0.1
[8]	4	12 × 10	30 × 30	26–30	24	82	<0.2
[9]	4	20 × 20	80 × 80	23–40	26	85	<0.01
[12]	4	15 × 10	20 × 20	27.5–28.5/37.5–38.5	24	80	<0.1
[16]	1	12 × 18	N/A	3–12	N/A	N/A	N/A
[17]	1	42 × 24	N/A	3–12	N/A	N/A	N/A
[18]	2	N/A	35 × 52	3.28–12	20	N/A	N/A
Proposed	4	10 × 12	24 × 24	24–39	26	92	<0.05

#### 4. Conclusions

This paper presented a novel, wideband, S-shape MIMO antenna with enhance isolation characteristics. The four-element MIMO antenna system showed isolation of  $-15$  dB, which with the help of an isolator, was improved to  $-26$  dB. The antenna is designed on  $0.254$  mm ultra-thin RO5880 substrate with relative permittivity of 2.3. The proposed antenna had compact dimensions of  $24 \times 24$  mm and the peak gain achieved was 7 dB, with bandwidth ranging between 25 and 40 GHz. The ECC value among any two radiating elements is less than 0.05, and efficiency is above 85% throughout the whole operating bandwidth. The fabricated prototype showed excellent agreement with simulations. Through valid measurement results, the proposed antenna is a suitable candidate for future mobile phones covering mmwave band and 5G high-data-rate devices.

**Author Contributions:** Conceptualization, A.G.A.H., M.A.K. and S.H.K.; methodology, M.A.K., A.G.A.H., E.M.A., M.A. and M.D.; software, M.E.M. and S.H.K.; validation, S.I.S., M.A.K. and A.N.N.; formal analysis, E.M.A., M.A. and M.D.; investigation, E.M.A., M.A. and M.D.; resources, A.N.N. and S.I.S.; data curation, S.H.K. and M.E.M.; writing—original draft preparation, M.A.K. and S.H.K.; writing—review and editing, S.H.K., J.I., M.A. and M.D.; visualization, J.I., M.A. and M.D.; supervision, A.N.N. and J.I.; project administration, S.H.K., M.A. and M.D.; funding acquisition, S.I.S., M.A. and M.D. All authors have read and agreed to the published version of the manuscript.

**Funding:** This project has received funding from Universidad Carlos III de Madrid and the European Union’s Horizon 2020 research and innovation programme under the Marie Skłodowska-Curie Grant 801538.

**Institutional Review Board Statement:** Not applicable.

**Informed Consent Statement:** Not applicable.

**Data Availability Statement:** All data have been included in the study.

**Conflicts of Interest:** The authors declare no conflict of interest.

#### References

1. Yang, Q.; Gao, S.; Luo, Q.; Wen, L.; Ban, Y.L.; Ren, X.; Wu, J.; Yang, X.; Liu, Y. Millimeter-wave dual-polarized differentially fed 2-D multibeam patch antenna array. *IEEE Trans. Antennas Propag.* **2020**, *68*, 7007–7016. [[CrossRef](#)]
2. Park, S.J.; Shin, D.H.; Park, S.O. Low side-lobe substrate-integrated-waveguide antenna array using broadband unequal feeding network for millimeter-wave handset device. *IEEE Trans. Antennas Propag.* **2015**, *64*, 923–932. [[CrossRef](#)]
3. Abdullah, M.; Kiani, S.H.; Iqbal, A. Eight element multiple-input multiple-output (MIMO) antenna for 5G mobile applications. *IEEE Access* **2019**, *7*, 134488–134495. [[CrossRef](#)]
4. Kiani, S.H.; Altaf, A.; Abdullah, M.; Muhammad, F.; Shoaib, N.; Anjum, M.R.; Damaševičius, R.; Blažauskas, T. Eight element side edged framed MIMO antenna array for future 5G smart phones. *Micromachines* **2020**, *11*, 956. [[CrossRef](#)] [[PubMed](#)]
5. Guo, J.; Cui, L.; Li, C.; Sun, B. Side-edge frame printed eight-port dual-band antenna array for 5G smartphone applications. *IEEE Trans. Antennas Propag.* **2018**, *66*, 7412–7417. [[CrossRef](#)]
6. Zhu, Q.; Ng, K.B.; Chan, C.H.; Luk, K.M. Substrate-integrated waveguide-fed array antenna covering 57–71 GHz band for 5G applications. *IEEE Trans. Antennas Propag.* **2017**, *65*, 6298–6306. [[CrossRef](#)]
7. Kamal, M.M.; Yang, S.; Ren, X.C.; Altaf, A.; Kiani, S.H.; Anjum, M.R.; Iqbal, A.; Asif, M.; Saeed, S.I. Infinity Shell Shaped MIMO Antenna Array for mm-Wave 5G Applications. *Electronics* **2021**, *10*, 165. [[CrossRef](#)]
8. Rahman, S.; Ren, X.C.; Altaf, A.; Irfan, M.; Abdullah, M.; Muhammad, F.; Anjum, M.R.; Mursal, S.N.F.; AlKahtani, F.S. Nature inspired MIMO antenna system for future mmWave technologies. *Micromachines* **2020**, *11*, 1083. [[CrossRef](#)] [[PubMed](#)]
9. Sehrai, D.A.; Abdullah, M.; Altaf, A.; Kiani, S.H.; Muhammad, F.; Tufail, M.; Irfan, M.; Glowacz, A.; Rahman, S. A Novel High Gain Wideband MIMO Antenna for 5G Millimeter Wave Applications. *Electronics* **2020**, *9*, 1031. [[CrossRef](#)]
10. Murthy, N. Improved isolation metamaterial inspired mm-Wave MIMO dielectric resonator antenna for 5G application. *Prog. Electromagn. Res. C* **2020**, *100*, 247–261. [[CrossRef](#)]
11. Sehrai, D.A.; Asif, M.; Shoaib, N.; Ibrar, M.; Jan, S.; Alibakhshikenari, M.; Lalbakhsh, A.; Limiti, E. Compact Quad-Element High-Isolation Wideband MIMO Antenna for mm-Wave Applications. *Electronics* **2021**, *10*, 1300. [[CrossRef](#)]
12. Raheel, K.; Altaf, A.; Waheed, A.; Kiani, S.H.; Sehrai, D.A.; Tubbal, F.; Raad, R. E-Shaped H-Slotted Dual Band mmWave Antenna for 5G Technology. *Electronics* **2021**, *10*, 1019. [[CrossRef](#)]
13. Kiani, S.H.; Altaf, A.; Anjum, M.R.; Afridi, S.; Arain, Z.A.; Anwar, S.; Khan, S.; Alibakhshikenari, M.; Lalbakhsh, A.; Khan, M.A.; et al. MIMO Antenna System for Modern 5G Handheld Devices with Healthcare and High Rate Delivery. *Sensors* **2021**, *21*, 7415. [[CrossRef](#)] [[PubMed](#)]

14. Luo, Y.; Shen, Y.; Cai, X.; Qian, F.; Xu, S.; Cui, H.; Yang, G. Substrate integrated coaxial line design for mmWave antenna with multilayer configuration. *Int. J. RF Microw. Comput. Aided Eng.* **2022**, *32*, e23090. [[CrossRef](#)]
15. Abdullah, M.; Kiani, S.H.; Abdulrazak, L.F.; Iqbal, A.; Bashir, M.A.; Khan, S.; Kim, S. High-performance multiple-input multiple-output antenna system for 5G mobile terminals. *Electronics* **2019**, *8*, 1090. [[CrossRef](#)]
16. Ojaroudi, M.; Ojaroudi, N.; Ghadimi, N. Dual band-notched small monopole antenna with novel coupled inverted U-ring strip and novel fork-shaped slit for UWB applications. *IEEE Antennas Wirel. Propag. Lett.* **2013**, *12*, 182–185. [[CrossRef](#)]
17. Mishra, S.K.; Gupta, R.K.; Vaidya, A.; Mukherjee, J. A compact dual-band fork-shaped monopole antenna for Bluetooth and UWB applications. *IEEE Antennas Wirel. Propag. Lett.* **2011**, *10*, 627–630. [[CrossRef](#)]
18. Dong, Y.; Li, Y.; Yu, K.; Wang, Y. *High Isolation Design of a Two-Element Planar UWB-MIMO Monopole Antenna*; International Applied Computational Electromagnetics Society Symposium: Firenze, Italy, 2017. [[CrossRef](#)]